Tailoring the atomic structure of graphene nanoribbons by scanning tunnelling microscope lithography

LEVENTE TAPASZTÓ[1]*, GERGELY DOBRIK[1], PHILIPPE LAMBIN[2] AND LÁSZLÓ P. BIRÓ[1]

[1]Research Institute for Technical Physics and Materials Science, H-1525 Budapest, Hungary
[2]Facultes Universitaire Notre Dame de la Paix, 61 Rue de Bruxelles, B-5000 Namur, Belgium
*e-mail: tapaszto@mfa.kfki.hu

Published online: 8 June 2008; doi:10.1038/nnano.2008.149

The practical realization of nanoscale electronics faces two major challenges: the precise engineering of the building blocks and their assembly into functional circuits[1]. In spite of the exceptional electronic properties of carbon nanotubes[2], only basic demonstration devices have been realized that require time-consuming processes[3–5]. This is mainly due to a lack of selective growth and reliable assembly processes for nanotubes. However, graphene offers an attractive alternative. Here we report the patterning of graphene nanoribbons and bent junctions with nanometre-precision, well-defined widths and predetermined crystallographic orientations, allowing us to fully engineer their electronic structure using scanning tunnelling microscope lithography. The atomic structure and electronic properties of the ribbons have been investigated by scanning tunnelling microscopy and tunnelling spectroscopy measurements. Opening of confinement gaps up to 0.5 eV, enabling room-temperature operation of graphene nanoribbon-based devices, is reported. This method avoids the difficulties of assembling nanoscale components and may prove useful in the realization of complete integrated circuits, operating as room-temperature ballistic electronic devices[6,7].

High electron mobility and long coherence length make graphene a subject of intense focus for nanoscale electronic applications, even for the realization of room-temperature ballistic (dissipation-free) electronics[8]. However, a major setback in the development of graphene-based field-effect transistors is the inability to electrostatically confine electrons in graphene, because a single layer of graphite remains metallic even at the charge neutrality point[9]. In order to overcome this problem, a way to open a gap in the electronic structure of graphene has to be found. A straightforward solution is to pattern the graphene sheet into narrow ribbons, which can be viewed as unrolled single-walled carbon nanotubes (CNTs). Owing to the quantum mechanical constriction of electronic wavefunctions in the direction perpendicular to the axis of the ribbon, a confinement-induced gap can open. Theoretical works have predicted that the width and crystallographic orientation of the graphene nanoribbons (GNRs) have a strong dependence on this gap[10,11], offering us the opportunity to tailor their electronic structure. However, it also imposes strict requirements on the fabrication of GNR-based devices, because in order to provide sufficient reproducibility, the accurate control of their structure with nanometre precision is of paramount importance.

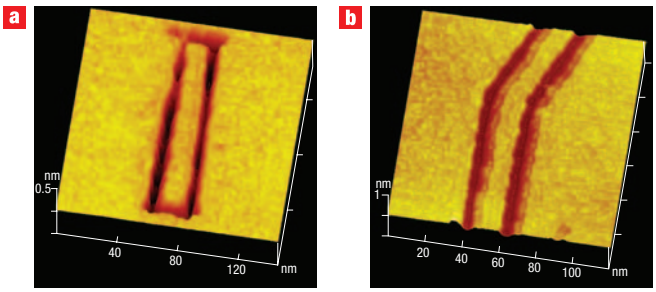

Figure 1 Graphene nanostructures patterned by STM lithography. **a**, 3D STM image of a 10-nm-wide and 120-nm-long graphene nanoribbon. **b**, An 8-nm-wide 30° GNR bent junction connecting an armchair and a zigzag ribbon.

With standard e-beam lithographic methods, GNRs down to a few tens of nanometres in width have been realized recently[12,13]; this seems to be the limit of this technique[1]. However, GNRs of just a few nanometres width are required to obtain energy gaps adequate for room-temperature operation, because the gap scales inversely with ribbon width[10,12]. It is obvious that this scale cannot be achieved by e-beam lithography. Moreover, electron lithographic methods have difficulties in controlling the crystallographic orientation of the ribbons.

Scanning probe microscopy techniques and in particular scanning tunnelling microscopy (STM) might offer the solution. STM combines the capability of atomic-resolution imaging with the ability to locally modify the surface of the samples[14]. The modification of the graphite surface by STM has an almost 20-year-old history[15]. However, previous works have focused on studying the mechanism of surface modification by analysing pit formation in graphite. Although the potential for etching lines has also been demonstrated[16], no further significant advance has been reported. In our work we combine the STM feature of surface modification with atomic-resolution imaging in order to engineer nanostructures with almost atomically precise structures and predetermined electronic properties.

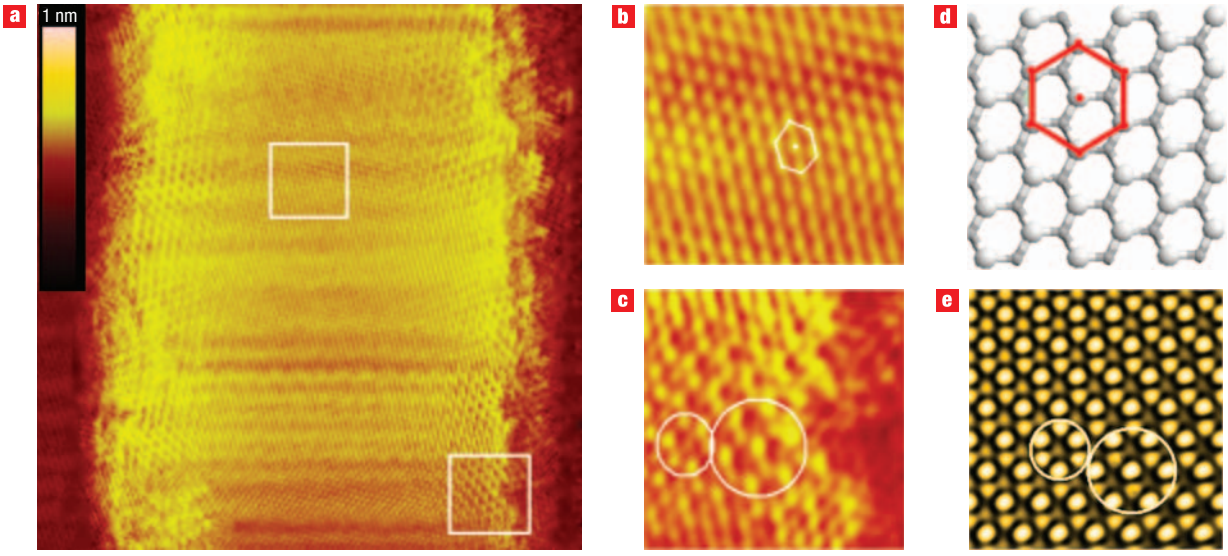

Figure 2 Atomic structure of GNRs. a, Atomic-resolution STM image (20 × 20 nm^2, 1 nA, 200 mV) of a 15-nm-wide GNR displaying an atomically flat and defect-free structure. The colour scale bars encode the height of the imaged features. **b**,**c**, Magnified images of the defect-free lattice taken at the centre of the ribbon (**b**) and position-dependent superstructures near the edges (**c**). **d**, Identification of crystallographic orientation from the triangular lattice observed in atomic-resolution STM images of HOPG-supported GNR. **e**, Theoretical STM image of the superstructures at the edges of the ribbon.

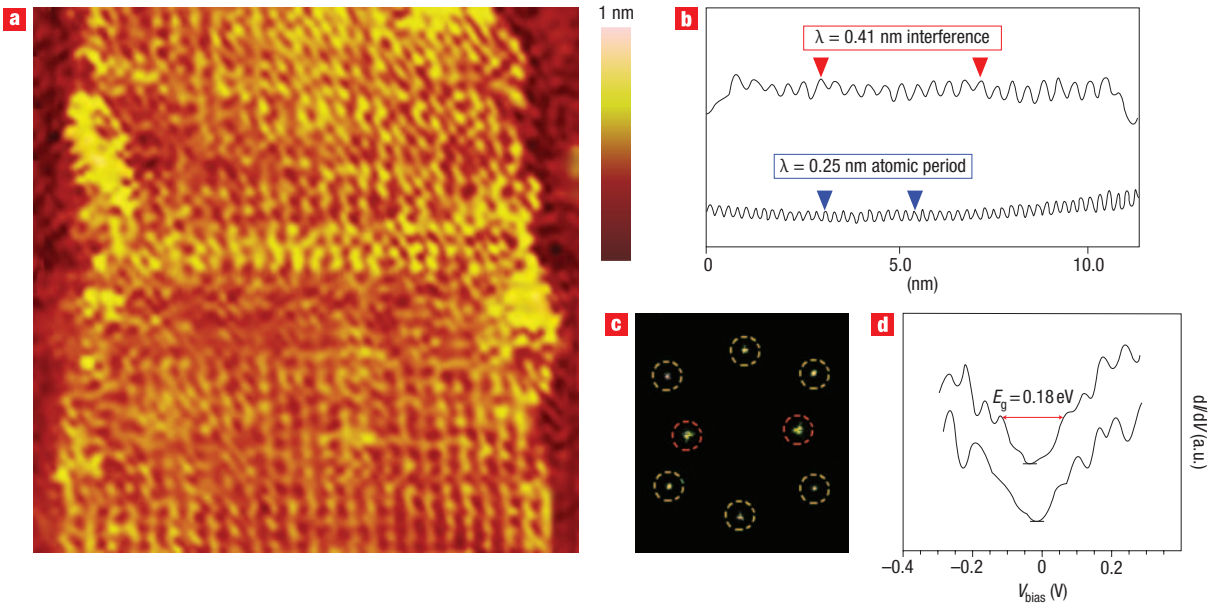

Figure 3 Electronic structure of GNRs. a, Constant-current STM image (12 × 12 nm^2, 1 nA, 100 mV) of a 10-nm-wide armchair GNR displaying confinement-induced standing electron wave patterns (stripes parallel to the axis of the ribbon). The colour scale bars encodes the height of the imaged features. **b**, Average line-cuts revealing the period of the observed oscillation, which clearly differs from the periodicity of the underlying atomic structure. **c**, 2D Fourier transformation of the STM image. **d**, Representative tunnelling spectra (STS) taken on the ribbon, revealing an energy gap of 0.18 eV (zero density of states (DOS) marked by horizontal lines).

Cutting of GNRs was carried out by applying a constant bias potential (significantly higher than the one used for imaging) and simultaneously moving the STM tip with constant velocity in order to etch the desired geometry fitted to the crystallographic structure, which was known from previous atomic-resolution STM imaging (see Methods for details).

Figure 1a shows a 10-nm-wide and 120-nm-long graphene nanoribbon etched by STM lithography. By setting the optimal lithographic parameters (2.4 V bias potential and 2.0 nm s^{-1} tip velocity) we were able to cut GNRs with suitably regular edges, which constitutes a great advance towards the reproducibility of GNR-based devices. Furthermore, more complex graphene nanoarchitectures can be tailored by STM lithography. As a basic demonstration, Fig. 1b shows an 8-nm-wide, 30° GNR bent junction connecting an armchair and a zigzag ribbon, giving rise to a metal–semiconductor molecular junction[7]. After the

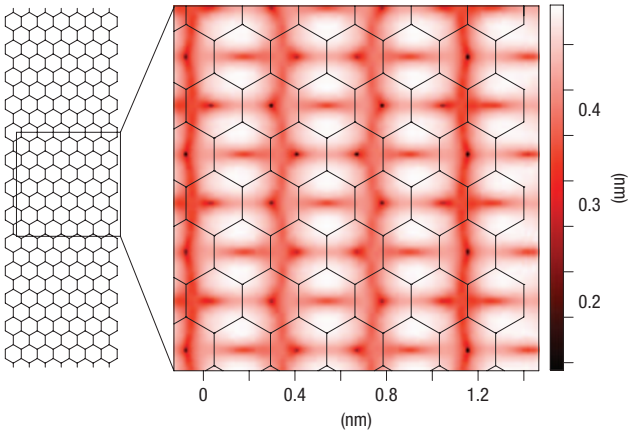

Figure 4 Tight-binding computation of the STM image of GNRs. Topographical STM image at constant current calculated for a 1.7-nm-wide armchair GNR at a tip potential $V_t = 0.5$ V and tip–GNR distance of 0.5 nm.

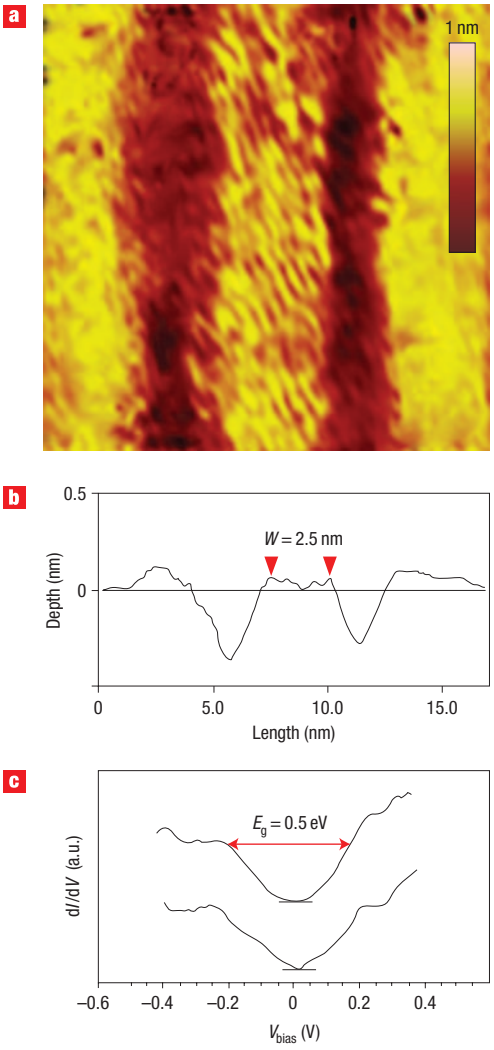

Figure 5 GNRs for room-temperature electronics. a, STM image (15×15 nm^2, 1 nA, 100 mV) of a 2.5-nm-wide armchair GNR. The colour scale bars encodes the height of the imaged features. **b**, Average line-cut of the STM image revealing the real width of the ribbon. **c**, Representative STS spectra taken on the narrow ribbon showing an energy gap of about 0.5 eV (zero DOS marked by horizontal lines).

patterning process, *in situ* atomic-resolution STM images could be achieved, revealing the atomic structure of the GNRs. The ribbon shown in Fig. 2a is ~15 nm wide and its axis has a crystallographic orientation close to the zigzag direction. The atomic-resolution image reveals an atomically flat and defect-free structure far from the edges, where a $\sqrt{3} \times \sqrt{3}\ R\ 30^\circ$ type superstructure pattern can be observed. The origin of this pattern is the interference of the electrons scattered at the irregularities of the edges[17,18] (Fig. 2e). For electronic device applications these ribbons have to be deposited on an insulating substrate. However, for atomic-resolution STM and scanning tunnelling spectroscopy (STS) investigation of GNRs, the surface of highly oriented pyrolytic graphite (HOPG) provides an ideal substrate, as it allows the ribbon to remain flat without inducing additional defects or changing its topology[19–21]. The intrinsic characteristics of GNRs can be studied this way.

When imaging a 10-nm-wide armchair GNR at low bias voltage (100 mV), oscillations in the electron density distribution parallel to the axis of the ribbon, reminiscent of a Fabry–Perot electron resonator, were observed, as shown in Fig. 3a. The periodicity of the observed oscillations was ~0.4 nm, which clearly differs from the period of the underlying atomic structure (0.246 nm), and corresponds to the Fermi wavelength of electrons in graphene (Fig. 3b). These findings are also supported by Fourier transformed images, which clearly indicate the presence of a lower frequency oscillation (red circles) than the atomic periodicity (yellow circles) in Fig. 3c. To correctly interpret the measurements we have performed theoretical modelling of STM images of GNRs based on a tight-binding π-electron Hamiltonian method[22]. Previously, the method has been used successfully in the interpretation of atomic-resolution STM images of CNTs. Figure 4 shows the calculated constant-current STM image of a 1.7-nm-wide armchair GNR. Stripes of high electron density distribution running parallel to the axis of the ribbon are clearly visible. The period of these oscillations is about 0.37 nm, which is close to the experimentally observed periodicity of 0.41 nm measured in Fig. 3. The small difference between the calculated and measured values might occur due to the doping of the GNR edges in air. At low bias voltages the STM measurements map the (square modulus of the) electronic wavefunction near the Fermi level[23], so we attribute these oscillations to the quantum mechanical confinement of electrons across the ribbon. The presence of continuous interference patterns along the whole length of the ribbon in the experimental images is spectacular evidence of phase-coherent quantum billiard (a standing electron wave) in GNRs at room temperature, which demonstrates their behaviour as electronic waveguides, even under ambient conditions. Both real and reciprocal space images (Fig. 3b,c, respectively) reveal a single characteristic oscillation period, indicating the one-dimensional (1D) nature of the electronic structure of the narrow GNRs. (See Supplementary Information, Figs S3 and S4, for bias-dependent and larger-area STM images, respectively.)

To experimentally investigate the electronic band structure of GNRs, STS measurements have been performed. Representative STS spectra taken on the 10-nm-wide armchair GNR are shown in Fig. 3d. The dI/dV quantity, which is proportional to the local electronic density of states (LDOS), revealed the presence of van Hove singularities, a signature of a 1D electronic structure, as is

well known for CNTs (ref. 24). (See Supplementary Information, Fig. S2, for a comparison with the LDOS of HOPG.) Furthermore, the distance between the first pair of van Hove singularities gives the value of the energy gap[24]. For the 10-nm-wide armchair GNR, a gap value of 0.18 eV was found, which seems to suit well the theoretical rule for separation of the energy levels due to the geometrical constriction of wavefunctions[25] $E_g(W) = \pi\hbar v_0/W \approx (2\,\mathrm{eV}\cdot\mathrm{nm})/W$, where W is the width of the ribbon and v_0 is the Fermi velocity of electrons in graphene. Our results concerning the electronic waveguide behaviour of GNRs are also in accordance with those derived from transport measurements[25,26] at low temperatures and for much wider ribbons.

Another advantage of STM lithography, beyond the precise engineering of the structure of GNRs, is the potential for downscaling. We were able to etch GNRs down to a width of 2.5 nm, corresponding to 10 carbon ring units along the width of the ribbon (Fig. 5a). The parameters used for lithography were 2.28 V bias potential and 1.0 nm s^{-1} tip velocity. The width and crystallographic orientation of the GNR shown in Fig. 5a correspond to an unrolled (10,0) zigzag single-walled CNT. The STS measurements performed on the 2.5-nm-wide ribbon shown in Fig. 5c reveal an energy gap of about 0.5 eV, in excellent agreement with first-principles theoretical calculations[11]. Tight binding calculations predict a gap of $1.2\,\mathrm{eV}\cdot\mathrm{nm}/W$, which is also in good agreement with our results. Furthermore, the gap value of 0.5 eV is comparable with that of Ge (0.67 eV), allowing the room-temperature operation of GNR-based electronic devices.

However, unlike CNTs, which are seamless graphitic structures rolled into a perfect cylinder, GNRs have edges. Because very narrow GNRs are needed to achieve the desired gap, the effect of edges can be critical. It has been shown theoretically that edge irregularities might induce electronic states within the gap region[27]. Our STM measurements also reveal oscillations in the electronic density of states (DOS) of the 2.5-nm-wide ribbon. These oscillations are less regular than the ones observed for wider ribbons; their orientation encloses a 30° angle with the ribbon axis, and the corresponding energy lies within the expected gap, which suggests that the imaged states are probably related to edge disorder.

Although SPM methods are usually characterized by low throughput, the manufacturing of large-scale integrated circuits of graphene by the SPM lithographic process presented above is not unrealistic, as 'Millipede'-type[28] scanning probe microscopes (SPM) are able to work in parallel, with more than 1,000 tips, which can significantly increase the efficiency.

In summary, we have developed an STM lithography-based technology that allows the engineering of graphene with true nanometre precision. We etched semiconducting ribbons from graphene with predetermined energy gap values up to 0.5 eV, allowing their operation at room temperature. These GNR devices also show a phase-coherent behaviour, even under ambient conditions. Furthermore, STM lithography offers us the opportunity for patterning more complicated architectures, even complete integrated circuits, from networks of GNRs. One can imagine the feasibility of a variety of electronic devices based on our technique, which could open up new directions in the experimental realization of graphene-based electronics.

METHODS

In order to pattern a single graphene sheet on the surface of a HOPG sample, we used a commercial DI Nanoscope III STM operating under ambient conditions. Pt–Ir tips proved to be the most suitable for both imaging and lithography. First, atomic-resolution images were taken on the atomically flat graphene sheet. The sample was then rotated in order to set the desired crystallographic orientation of the ribbon axis (edges), and the graphene layer was cut by applying a constant bias potential (significantly higher than the one used for imaging) and simultaneously moving the STM tip with constant velocity in order to etch the desired geometry. Good results were obtained for positive sample biases. The microscopic mechanism of etching is not yet fully understood. Most likely the breaking of carbon–carbon bonds by field-emitted electrons combined with the electron-transfer-enhanced oxidation of the graphene is responsible for the etching[29]. The whole lithographic process was controlled by a custom-written computer code enabling us to manage several parameters. The applied bias potential and the velocity of the tip during patterning were found to be the critical parameters. The optimal parameters were slightly dependent on the microstructure of the mechanically etched tips, but typically varied in the range of 2.2–2.6 V for the bias voltages and 1.0–5.0 nm s^{-1} for the tip velocities. Here we note that during the patterning we used tip velocities that were three orders of magnitude lower than those reported in ref. 16, and moved the tip only once along the lines to be etched, instead of scanning it several hundred times with high velocity. After optimizing the parameters of the lithographic process we were able to cut single-layer trenches (0.335 nm deep), down to a width of 1 nm, and several hundreds of nanometres long, with well-defined edges. (See Supplementary Information, Fig. S1, for experimental evidence of patterning only a single graphene layer.) The STM lithographic patterning showed good stability and reproducibility, even under ambient conditions. After several etching processes the quality of the STM tip was still good enough to achieve atomic-resolution images of the GNRs, enabling us to investigate *in situ* their atomic structure.

Received 16 January 2008; accepted 1 May 2008; published 8 June 2008.

References

1. Avouris, P., Chen, Z. & Perebeinos, V. Carbon-based electronics. *Nature Nanotech.* **2,** 605–615 (2007).
2. Avouris, P. Molecular electronics with carbon nanotubes. *Acc. Chem. Res.* **35,** 1026–1034 (2002).
3. Tans, S. J., Verschueren, A. R. M. & Dekker, C. Room-temperature transistor based on a single carbon nanotube. *Nature* **393,** 49–52 (1998).
4. Yao, Z., Postma, H. W. C., Balents, L. & Dekker, C. Carbon nanotube intramolecular junctions. *Nature* **402,** 273–276 (1999).
5. Keren, K., Berman, R. S., Buchstab, E., Sivan, U. & Braun, E. DNA-templated carbon nanotube field-effect transistor. *Science* **302,** 1380–1382 (2003).
6. Areshkin, D. A. & White, C. T. Building blocks for integrated graphene circuits. *Nano Lett.* **7,** 3253–3259 (2007).
7. Yan, Q. *et al.* Intrinsic current–voltage characteristics of graphene nanoribbon transistors and effect of edge doping. *Nano Lett.* **7,** 1469–1473 (2007).
8. Geim, A. K. & Novoselov, K. S. The rise of graphene. *Nature Mater.* **6,** 183–191 (2007).
9. Novoselov, K. S. *et al.* Two-dimensional gas of massless Dirac fermions in graphene. *Nature* **438,** 197–200 (2005).
10. Barone, V., Hod, O. & Scuseria, G. E. Electronic structure and stability of semiconducting graphene nanoribbons. *Nano Lett.* **6,** 2748–2754 (2006).
11. Son, Y. W., Cohen, M. L. & Louie, S. G. Energy gaps in graphene nanoribbons. *Phys. Rev. Lett.* **97,** 216803 (2006).
12. Han, M. Y., Ozylmaz, B., Zhang, Y. & Kim, P. Energy band-gap engineering of graphene nanoribbons. *Phys. Rev. Lett.* **98,** 206805 (2007).
13. Chen, Z., Lin, Y. M., Rooks, M. J. & Avouris, P. Graphene nano-ribbon electronics. *Physica E* **40,** 228–232 (2007).
14. Tseng, A. A., Notargiacomo, A. & Chen, T. P. Nanofabrication by scanning probe microscope lithography: A review. *J. Vac. Sci. Technol. B* **23,** 877–894 (2005).
15. Albrecht, T. R. *et al.* Nanometer-scale hole formation on graphite using a scanning tunneling microscope. *Appl. Phys. Lett.* **55,** 1727–1729 (1989).
16. McCarley, R. L., Hendricks, S. A. & Bard, A. J. Controlled nanofabrication of highly oriented pyrolytic graphite with the scanning tunneling microscope. *J. Phys. Chem.* **96,** 10089–10092 (1992).
17. Mizes, H. A. & Foster, J. S. Long-range electronic perturbations caused by defects using scanning tunneling microscopy. *Science* **244,** 559–562 (1989).
18. Tapasztó, L. *et al.* Electron scattering in a multiwall carbon nanotube bend junction studied by scanning tunneling microscopy. *Phys. Rev. B* **74,** 235422 (2006).
19. Ishigami, M., Chen, J. H., Cullen, W. G., Fuhrer, M. S. & Williams, E. D. Atomic structure of graphene on SiO_2. *Nano Lett.* **7,** 1643–1648 (2007).
20. Rutter, G. M. *et al.* Scattering and interference in epitaxial graphene. *Science* **317,** 219–222 (2007).
21. Gomez-Navarro, C. *et al.* Electronic transport properties of individual chemically reduced graphene oxide sheets, *Nano Lett.* **7,** 3499–3503 (2007).
22. Meunier, V. & Lamnin, P. Tight-binding computation of the STM image of carbon nanotubes. *Phys. Rev. Lett.* **81,** 5588–5591 (1998).
23. Tersoff, J. & Hamann, D. R. Theory of the scanning tunneling microscope. *Phys. Rev. B* **31,** 805–813 (1985).
24. Wildöer, J. W. G., Venema, L. C., Rinzler, A. G., Smalley, R. E. & Dekker, C. Electronic structure of atomically resolved carbon nanotubes. *Nature* **391,** 59–62 (1998).
25. Berger, C. *et al.* Electronic confinement and coherence in patterned epitaxial graphene. *Science* **312,** 1191–1196 (2006).
26. Miao, F. *et al.* Phase-coherent transport in graphene quantum billiards. *Science* **317,** 1530–1533 (2007).
27. Yoon, Y. & Guo, J. Effect of edge roughness in graphene nanoribbon transistors. *Appl. Phys. Lett.* **91,** 73103 (2007).
28. Knoll, A. *et al.* Integrating nanotechnology into a working storage device. *Microelectron. Eng.* **83,** 1692–1697 (2006).

29. Kim, D. H., Koo, J. Y. & Kim, J. J. Cutting of multiwalled carbon nanotubes by a negative voltage tip of an atomic force microscope: A possible mechanism. *Phys. Rev. B* **68,** 113406 (2003).

Supplementary information accompanies this paper on www.nature.com/naturenanotechnology.

Acknowledgements

This work was supported in Hungary by OTKA (Országos Tudományos Kutatási Alapprogramok) grant 67851 and OTKA-NKTH (Nemzeti Kutatási és Technológiai Hivatal) grant K67793.

Author contributions

L.T. conceived the experiments. L.T. and G.D. performed the experiments. L.T., P.L. and L.P.B. analysed the data. L.T. wrote the paper. All authors discussed the results and commented on the manuscript.

Author information

Reprints and permission information is available online at http://npg.nature.com/reprintsandpermissions/. Correspondence and requests for materials should be addressed to L.T.